CEAI, Vol.15, No.1 pp. 63-70, 2013 Printed in Romania

Line-of-sight stabilization by robust L_1 controller based on Linear Matrix Inequality (LMI) approach

Ali Akbar Jalali, Hassan Golmohammad

Electrical Engineering Department,
Iran University of Science and Technology (IUST), Narmak 16846-13114, Tehran, Iran
(e-mail: 86814024@ee.iust.ac.ir, drjalali@iust.ac.ir)
(Tel: +98-21-77240492; Fax: +98-21-77240490)

Abstract: Vibration reduces the ability of a camera to detect far-away targets that lead to the use of stabilized platforms. Despite much research on stabilized platforms, the need of more accurate systems still exists as a consequence of sensor resolution improvements. The stabilization problem is the problem of attenuating persistent disturbances which is a suitable case-study for $\mathbf{L_1}$ control problem. In this article, a robust $\mathbf{L_1}$ controller is designed for a nonlinear gyro-stabilized system based on LMI approach. The performance of the introduced controller is evaluated by simulation and is compared with a robust $\mathbf{H}_\infty$ controller. Using the proposed approach, the stability accuracy of the platform improves significantly.

Keywords: $\mathbf{L_1}$control, Linear Matrix Inequality, line-of-sight stabilization, gyroscope.

1. INTRODUCTION

Sometimes in practical applications exogenous inputs like disturbances or noise, are encountered which are persistent in nature and the only information available about these signals is their peak amplitude. The $\mathcal{L}_\infty$-norm provides a suitable way to characterize the effect of such signals. It can be used to capture the peak amplitude of certain output signals in a control system design problem. For instance in the line-of-sight stabilization problem, the design specification imposes an upper bound on the peak value of the platform angle deviation, i.e. the output, during persistent disturbances. Also, since the plant (the actuator) normally has a maximum input rating, the output of the controller has to be bounded in amplitude in order to avoid saturation of the plant. Such constraints can be captured by the $\mathcal{L}_\infty$-norm of the transfer function from the input to the output signal of interest.

Design of a stabilized line-of-sight is a well-known problem, and most of its tradeoffs have been identified. Historically, the first stabilized platform is a stabilized head mirror system introduced on fire control systems in the late 1970s, but the system was costly for the performance achieved (Ortega 1999). Despite much research on stabilized platforms, the need of more accurate systems still exists as a consequence of sensor resolution improvements (Hilkert 2008).

Numerous control algorithms have been applied for line-of-sight stabilization. Rue paved the way for line-of-sight stabilization. He used a linear controller and measured the stability accuracy by frequency domain criterion (Rue 1969, 1974). Li et al. used a Linear Quadratic Gaussian (LQG) controller combined with an online identifier to compensate friction effects based on first-order stochastic differential equation. Performance of the controller was compared with a Proportional-plus-Integral (PI) controller with a notch filter (Li 1998a, 1998b). Rezac et al. designed an accurate system by considering LuGre friction model and feedforward compensator (Rezac 2011). A two-axis gimbal system has been satisfactorily stabilized by a Loop Transfer Recovery (LTR) controller (Seong 2006). Intelligent controllers like fuzzy and neural networks algorithms are also used for line-of-sight stabilization (Ji 2011, Moorty 2004, Lee 1998). Controllers designed based on fractional-order theory operate well for line-of-sight stabilization, too (Wang 2008). There are two approaches in line-of-sight stabilization: direct and indirect line-of-sight stabilization (Kennedy 2003). In all the reviewed articles, direct approach has been adopted for line-of-sight stabilization and the stabilization problem is treated as a traditional control problem. It means that the controller is designed mentioning closed-loop specifications like rise-time, overshoot and bandwidth. In this article, an L_1 controller is going to be designed for a gyro-stabilized platform. The nature of the stabilization problem, i.e. imposing a limit on the peak value of the output, will be encountered in the design procedure, too.

In this article, the L_1 control problem will be solved by Linear Matrix Inequalities (LMIs). The current work is the modified version of (Khosravi 2008). The last LMI formulation for the L_1 control problem was based on solving three LMIs simultaneously which are alternative LMIs for two original LMIs. The link between original LMIs and the alternative ones are only sufficient. Therefore, it covers limited number of L_1 control problems and the designer has no option when the alternative LMIs are not solvable. In the current LMI formulation for the L_1 control problem, an additional LMI is added to the formulation to make the link necessary and sufficient. In addition, the analysis and synthesis steps are completely separated using the added LMI. As a result, the designer has a criterion to change the design constraints via weighting functions when the analysis LMIs are not solvable.

This article is divided into five sections. Section two describes the general framework for the analysis and synthesis of the controller based on the LMI approach. The platform is described in section three where the controller is designed. The utility of the approach is illustrated in section four by simulation. The robust L_1 controller is design using the introduced approach and compared with a robust H_∞ controller designed by the same weighing functions. As a result, the stability accuracy of the platform improves significantly. Finally, section five contains some conclusions.

2. LMI CONSTRAINTS FOR L_1 CONTROLLER

Consider the system

$$\begin{cases} \dot{x} = \hat{A}x + \hat{B}w \\ z = \hat{C}x + \hat{D}w \end{cases} \tag{1}$$

where $x(t) \in \mathbb{R}^n$ is the state, $w(t) \in \mathbb{R}^{n_w}$ the input and $z(t) \in \mathbb{R}^{n_z}$ the output. Assume that the system is stable. For the fixed initial condition $x(0) = 0$ the system defines a mapping from bounded-amplitude inputs $w \in \mathcal{L}_\infty$ to bounded-amplitude outputs $z \in \mathcal{L}_\infty$ and a relevant performance criterion is the peak-to-peak or $\mathcal{L}_\infty$-induced norm of this mapping

$$\|T_{zw}\|_{\infty,\infty} := sup_{0<\|w\|_\infty<\infty} \frac{\|z\|_\infty}{\|w\|_\infty} \tag{2}$$

The following lemma gives a sufficient condition for an upper bound γ_1 of the peak-to-peak gain of the system.

Lemma 1: If there exists $\hat{X} > 0$, $\lambda > 0$ and $\mu > 0$ such that

$$\begin{pmatrix} \hat{A}^T\hat{X} + \hat{X}\hat{A} + \lambda\hat{X} & \hat{X}\hat{B} \\ \hat{B}^T\hat{X} & -\mu I \end{pmatrix} < 0 \tag{3}$$

$$\begin{pmatrix} \lambda\hat{X} & 0 & \hat{C}^T \\ 0 & (\gamma_1 - \mu)I & \hat{D}^T \\ \hat{C} & \hat{D} & \gamma_1 I \end{pmatrix} > 0 \tag{4}$$

then the peak-to-peak norm (or $\mathcal{L}_\infty$-induced norm) of the system is smaller than γ_1, i.e. $\|T_{zw}\|_{\infty,\infty} < \gamma_1$.

Proof: See (Sherer 2004).

Assume the generalized plant

$$\begin{pmatrix} \dot{x} \\ z \\ y \end{pmatrix} = \begin{pmatrix} A & B_w & B \\ C_z & D_{zw} & D_z \\ C & D_w & 0 \end{pmatrix} \begin{pmatrix} x \\ w \\ u \end{pmatrix} \tag{5}$$

and the controller

$$\begin{pmatrix} \dot{\varepsilon} \\ u \end{pmatrix} = \left(\begin{array}{c|c} A_K & B_K \\ \hline C_K & D_K \end{array}\right) \begin{pmatrix} \varepsilon \\ y \end{pmatrix} \tag{6}$$

where the pair (A, B) is controllable and the pair (A, C) is detectable and $A_K \in \mathbb{R}^{n_k \times n_k}$. The matrices of the closed-loop system are

$$\left(\begin{array}{c|c} A_{cl} & B_{cl} \\ \hline C_{cl} & D_{cl} \end{array}\right) = \left(\begin{array}{cc|c} A+BD_KC & BC_K & B_w+BD_KD_w \\ B_KC & A_K & B_KD_w \\ \hline C_z+D_zD_KC & D_zC_K & D_{zw}+D_zD_KD_w \end{array}\right) \tag{7}$$

The control design problem is to find the dynamic control law (6) that satisfies certain set of specifications on the general transfer function described by equation (5). These set of specifications are captured by weighted system norms.

Gathering all controller parameters into the single variable

$$\hat{K} = \left(\begin{array}{c|c} A_K & B_K \\ \hline C_K & D_K \end{array}\right) \tag{8}$$

and introducing the following short-hands (from (Gahinet 1994))

$$\overline{A} = \begin{pmatrix} A & 0 \\ 0 & 0_{n_k} \end{pmatrix}, \quad \overline{B} = \begin{pmatrix} B_w \\ 0 \end{pmatrix}, \quad \overline{C} = \begin{pmatrix} C_z & 0 \end{pmatrix}$$

$$\underline{B} = \begin{pmatrix} 0 & B \\ I_{n_k} & 0 \end{pmatrix}, \underline{C} = \begin{pmatrix} 0 & I_{n_k} \\ C & 0 \end{pmatrix},$$

$$\underline{D_z} = \begin{pmatrix} 0 & D_z \end{pmatrix}, \quad \underline{D_w} = \begin{pmatrix} 0 \\ D_w \end{pmatrix}$$

the closed-loop matrices can be rewritten as:

$$A_{cl} = \overline{A} + \underline{B}\hat{K}\underline{C},$$
$$B_{cl} = \overline{B} + \underline{B}\hat{K}\underline{D_w},$$
$$C_{cl} = \overline{C} + \underline{D_z}\hat{K}\underline{C},$$
$$D_{cl} = D_{zw} + \underline{D_z}\hat{K}\underline{D_w}$$

Note these equations involve only plant data and that the closed-loop matrices depend affinely on the controller $\hat{K}$.

LMI (3) can be rewritten for the closed-loop plant as

$$\begin{pmatrix} A_{cl}^T X_{cl} + X_{cl}A_{cl} + \lambda X_{cl} & X_{cl}B_{cl} \\ B_{cl}^T X_{cl} & -\mu I \end{pmatrix} < 0 \tag{9}$$

$$\Rightarrow H_{X_{cl}} + Q^T\hat{K}^T P_{X_{cl}} + P_{X_{cl}}^T \hat{K} Q < 0 \tag{10}$$

where

$$H_{X_{cl}} = \begin{pmatrix} \overline{A}^T X_{cl} + X_{cl}\overline{A} + \lambda X_{cl} & X_{cl}\overline{B} \\ \overline{B}^T X_{cl} & -\mu I \end{pmatrix},$$

$$P_{X_{cl}} = \begin{pmatrix} \underline{B}^T X_{cl} & 0 \end{pmatrix}, \quad Q = \begin{pmatrix} \underline{C} & \underline{D_w} \end{pmatrix}$$

Let $N_{P_{X_{cl}}}$ and N_Q denote matrices whose columns form bases for the null-space of $P_{X_{cl}}$ and the null-space of Q, respectively. It has been proved that LMI (10) is solvable for $\hat{K}$ if and only if the two inequalities

$$N_P^T T_{X_{cl}} N_P < 0 \tag{11}$$

and

$$N_Q^T H_{X_{cl}} N_Q < 0 \tag{12}$$

are satisfied (Khosravi 2008), where

$$T_{X_{cl}} = \begin{pmatrix} \overline{A}X_{cl}^{-1} + X_{cl}^{-1}\overline{A}^T + \lambda X_{cl}^{-1} & \overline{B} \\ \overline{B}^T & -\mu I \end{pmatrix}$$

$$P = \begin{pmatrix} \underline{B}^T & 0 \end{pmatrix}$$

In inequalities (11) and (12), the controller parameters $\hat{K}$ is eliminated.

Inequalities (11) and (12) contain both X_{cl} and X_{cl}^{-1}. Let partition X_{cl} and X_{cl}^{-1} as follows

$$X_{cl} = \begin{pmatrix} X & X_2 \\ X_2^T & X_3 \end{pmatrix}, \quad X_{cl}^{-1} = \begin{pmatrix} Y & Y_2 \\ Y_2^T & Y_3 \end{pmatrix} \tag{13}$$

Lemma 2 states LMIs (11) and (12) with respect to X and Y matrices.

Lemma 2: Inequalities (11) and (12) are satisfied if and only if the following inequalities are satisfied

$$\begin{pmatrix} Y & I \\ I & X \end{pmatrix} > 0 \tag{14}$$

$$N_O^T \begin{pmatrix} \overline{A}^T X + X\overline{A} + \lambda X & X\overline{B} \\ \overline{B}^T X & -\mu I \end{pmatrix} N_O < 0 \tag{15}$$

$$N_C^T \begin{pmatrix} \overline{A}Y + Y\overline{A}^T + \lambda Y & \overline{B} \\ \overline{B}^T & -\mu I \end{pmatrix} N_C < 0 \tag{16}$$

where N_O and N_C are matrices whose columns form bases for the null-space of $\begin{pmatrix} 0 & 0 \\ C & D_w \end{pmatrix}$ and the null-space of $\begin{pmatrix} 0 & 0 \\ B^T & 0 \end{pmatrix}$, respectively.

Proof: See (Khosravi 2008).

Lemma 2 modifies inequality (3) to eliminate the controller parameters. The next theorem eliminates the controller parameters form inequality (4). As a result, one can solve inequalities (3) and (4) without unknown parameter $\widehat{K}$.

Theorem 1: For the generalized plant (5) and the controller (6), the inequality

$$\begin{pmatrix} \lambda X_{cl} & 0 & C_{cl}^T \\ 0 & (\gamma_1 - \mu)I_{n_w} & D_{cl}^T \\ C_{cl} & D_{cl} & \gamma_1 I_{n_z} \end{pmatrix} > 0 \tag{17}$$

is satisfied if and only if

$$\begin{pmatrix} N_O & 0 \\ 0 & I_{n_z} \end{pmatrix}^T \begin{pmatrix} \lambda X & 0 & C_z^T \\ 0 & (\gamma_1 - \mu)I_{n_w} & D_{zw}^T \\ C_z & D_{zw} & \gamma_1 I_{n_z} \end{pmatrix} \begin{pmatrix} N_O & 0 \\ 0 & I_{n_z} \end{pmatrix} > 0 \tag{18}$$

where N_O is defined in lemma 2.

Proof:

Necessity: Taking a Schur complement of inequality (17) yields that

$$\begin{pmatrix} \lambda X_{cl} & 0 \\ 0 & (\gamma_1 - \mu)I_{n_w} \end{pmatrix} - \frac{1}{\gamma_1}\begin{pmatrix} C_{cl}^T \\ D_{cl}^T \end{pmatrix}\begin{pmatrix} C_{cl} & D_{cl} \end{pmatrix} > 0 \tag{19}$$

Assuming

$$S = \begin{pmatrix} \overline{C} & D_{zw} \end{pmatrix} \tag{20}$$

one has

$$\begin{pmatrix} \lambda X_{cl} & 0 \\ 0 & (\gamma_1 - \mu)I_{n_w} \end{pmatrix} - \frac{1}{\gamma_1} S^T S - \frac{1}{\gamma_1}\begin{pmatrix} Q^T \widehat{K}^T \underline{D_z^T} & I \end{pmatrix}\begin{pmatrix} I & S \\ S^T & 0 \end{pmatrix}\begin{pmatrix} \underline{D_z}\widehat{K}Q \\ I \end{pmatrix} > 0 \tag{21}$$

By pre- and post-multiplying the inequality by N_Q^T and N_Q, respectively, the controller parameter $\widehat{K}$ is eliminated and the inequality reduces to

$$N_Q^T \begin{pmatrix} \lambda X_{cl} & 0 \\ 0 & (\gamma_1 - \mu)I_{n_w} \end{pmatrix} N_Q - \frac{1}{\gamma_1} N_Q^T S^T S N_Q > 0 \tag{22}$$

The matrix N_Q has a form like

$$N_Q = \begin{pmatrix} N_{Q1} & N_{Q2} \\ 0 & 0 \\ N_{Q3} & N_{Q4} \end{pmatrix} \tag{23}$$

Because

$$Q = \begin{pmatrix} \underline{C} & \underline{D_w} \end{pmatrix} = \begin{pmatrix} 0 & I_{n_k} & 0 \\ C & 0 & D_w \end{pmatrix} \tag{24}$$

Using adequate partitions and mentioning matrix dimensions, one has

$$SN_Q = \begin{pmatrix} C_z & 0 & D_{zw} \end{pmatrix}\begin{pmatrix} N_{Q1} & N_{Q2} \\ 0 & 0 \\ N_{Q3} & N_{Q4} \end{pmatrix} =$$

$$\begin{pmatrix} C_z & D_{zw} \end{pmatrix}\begin{pmatrix} N_{Q1} & N_{Q2} \\ N_{Q3} & N_{Q4} \end{pmatrix} = \begin{pmatrix} C_z & D_{zw} \end{pmatrix} N_O \tag{25}$$

and

$$N_Q^T \begin{pmatrix} \lambda X_{cl} & 0 \\ 0 & (\gamma_1 - \mu)I_{n_w} \end{pmatrix} N_Q$$

$$= \begin{pmatrix} N_{Q1} & N_{Q2} \\ 0 & 0 \\ N_{Q3} & N_{Q4} \end{pmatrix}^T \begin{pmatrix} \lambda X & \lambda X_2 & 0 \\ \lambda X_2 & \lambda X_3 & 0 \\ 0 & 0 & (\gamma_1 - \mu)I_{n_w} \end{pmatrix}\begin{pmatrix} N_{Q1} & N_{Q2} \\ 0 & 0 \\ N_{Q3} & N_{Q4} \end{pmatrix}$$

$$\Rightarrow \begin{pmatrix} N_{Q1} & N_{Q2} \\ N_{Q3} & N_{Q4} \end{pmatrix}^T \begin{pmatrix} \lambda X & 0 \\ 0 & (\gamma_1 - \mu)I_{n_w} \end{pmatrix}\begin{pmatrix} N_{Q1} & N_{Q2} \\ N_{Q3} & N_{Q4} \end{pmatrix} =$$

$$N_O^T \begin{pmatrix} \lambda X & 0 \\ 0 & (\gamma_1 - \mu)I_{n_w} \end{pmatrix} N_O \tag{26}$$

Replacing (25) and (26) in (22), one has

$$N_O^T \begin{pmatrix} \lambda X & 0 \\ 0 & (\gamma_1 - \mu)I_{n_w} \end{pmatrix} N_O - \frac{1}{\gamma_1} N_O^T \begin{pmatrix} C_z & D_{zw} \end{pmatrix}^T \begin{pmatrix} C_z & D_{zw} \end{pmatrix} N_O > 0$$

$\Rightarrow$

$$N_O^T \begin{pmatrix} \lambda X & 0 \\ 0 & (\gamma_1 - \mu)I_{n_w} \end{pmatrix} N_O - \frac{1}{\gamma_1}\left(\begin{pmatrix} C_z & D_{zw} \end{pmatrix} N_O\right)^T \begin{pmatrix} C_z & D_{zw} \end{pmatrix} N_O > 0 \tag{27}$$

It can be represented in an LMI form using the Schur complement as

$$\begin{pmatrix} N_O^T \begin{pmatrix} \lambda X & 0 \\ 0 & (\gamma_1 - \mu)I_{n_w} \end{pmatrix} N_O & N_O^T \begin{pmatrix} C_z & D_{zw} \end{pmatrix}^T \\ \begin{pmatrix} C_z & D_{zw} \end{pmatrix} N_O & \gamma_1 I_{n_z} \end{pmatrix} > 0 \tag{28}$$

$$\Rightarrow \begin{pmatrix} N_O^T & 0 \\ 0 & I_{n_z} \end{pmatrix}\begin{pmatrix} \lambda X & 0 & C_z^T \\ 0 & (\gamma_1 - \mu)I_{n_w} & D_{zw}^T \\ C_z & D_{zw} & \gamma_1 I_{n_z} \end{pmatrix}\begin{pmatrix} N_O & 0 \\ 0 & I_{n_z} \end{pmatrix} > 0$$

which is the proposed result.

Sufficiency: Inequality (19) can be rewritten as

$$\Psi + Q^T\Lambda + \Xi Q > 0 \tag{29}$$

where

$$\Psi = \begin{pmatrix} \lambda X_{cl} & 0 \\ 0 & (\gamma_1 - \mu)I_{n_w} \end{pmatrix} - \frac{1}{\gamma_1}S^TS$$

$$\Lambda = \hat{K}^T\underline{D_z^T}\,\underline{D_z}\hat{K}Q + \hat{K}^T\underline{D_z^T}\,S$$

$$\Xi = S^T\underline{D_z}\hat{K}$$

Assuming that

$$\Phi = (N_Q \quad V) \tag{30}$$

is a complete basis for $\mathbb{R}^{n+n_k+n_w}$ and pre- and post-multiplying the inequality by Φ^T and Φ, respectively, inequality (29) is equivalent to

$$\Phi^T\Psi\Phi + \Phi^TQ^T\Lambda\Phi + \Phi^T\Xi Q\Phi > 0 \tag{31}$$

Let partitions matrices as

$$Q\Phi = Q(N_Q \quad V) = (0 \quad QV) \tag{32}$$

and

$$\Phi^T\Psi\Phi = \begin{pmatrix} N_Q^T\Psi N_Q & N_Q^T\Psi V \\ V^T\Psi N_Q & V^T\Psi V \end{pmatrix} = \begin{pmatrix} \Psi_1 & \Psi_2 \\ \Psi_2^T & \Psi_3 \end{pmatrix} \tag{33}$$

The equality

$$\Phi^TQ^T\Lambda\Phi + \Phi^T\Xi Q\Phi = \begin{pmatrix} 0 & \Theta_2 \\ \Theta_2^T & \Theta_3 \end{pmatrix} \tag{34}$$

is achieved as a result of (32). Using (33) and (34), inequality (31) becomes

$$\begin{pmatrix} \Psi_1 & \Psi_2 + \Theta_2 \\ \Psi_2^T + \Theta_2^T & \Psi_3 + \Theta_3 \end{pmatrix} > 0 \tag{35}$$

By a Schur complement argument, inequality (35) is satisfied if and only if

$$\Psi_1 > 0 \tag{36}$$

and

$$\Psi_3 + \Theta_3 - (\Psi_2 + \Theta_2)^T\Psi_1^{-1}(\Psi_2 + \Theta_2) > 0 \tag{37}$$

Given Θ_2, one can always find Θ_3 such that (37) is satisfied. Hence (29) is feasible if and only if (36) is feasible. The condition (36) is exactly (22).

Note that in proof of the sufficiency of the theorem, matrix Φ is an inversable matrix while N_Q is not an inversable matrix so one can achieve (29) from (31) by pre- and post-multiplying the inequality by ${\Phi^{-1}}^T$ and Φ^{-1}, respectively.

In order to synthesize the controller, X_{cl} should be calculated to solve LMIs for controller parameters $\hat{K}$. Considering a full-order controller i.e. $n = n_k$, one has

$$X_{cl}X_{cl}^{-1} = \begin{pmatrix} X & X_2 \\ X_2^T & X \end{pmatrix}\begin{pmatrix} Y & Y_2 \\ Y_2^T & Y \end{pmatrix} = I \tag{38}$$

Then

$$X_2^TX^{-1}X_2 = X - Y^{-1} \tag{39}$$

so

$$X_2 = X^{\frac{1}{2}}(X - Y^{-1})^{\frac{1}{2}} \tag{40}$$

and consequently

$$X_{cl} = \begin{pmatrix} X & X_2 \\ X_2^T & X \end{pmatrix} \tag{41}$$

Note that Y is always inversable because $Y > 0$. If $n_k < n$ the problem is more difficult. The interested reader may review reference (Packard 1991) lemma 7.5 for an additional condition.

The algorithm contains the following steps:

Step 1: (Analysis Step) Using a fixed $\lambda > 0$ solve LMIs (14), (15), (16) and (18) simultaneously for the generalized plant (5). If the LMIs are solvable then X, Y, μ and γ_1 are achieved.

Step 2: Compute X_{cl} using equation (41).

Step 3: (Synthesis Step) Solve the LMIs (10) and (17) using achieved values in previous steps to achieve the controller $\hat{K}$.

Step 4: To find the optimal controller, find the minimum value of $\gamma_1(\lambda)$ using a linear search over λ and repeating steps one through three.

3. ROBUST L1 CONTROLLER

In this section, the proposed controller is designed for the speed loop shown in Figure1.

Figure 2 illustrates a typical gyro-stabilized system with nonlinear functions. This block diagram is similar to the gyro-stabilized system used in (Moorty 2004). It contains a dc torque motor, driver, gimbal and gyroscope model. Nonlinearities are modelled using two saturation blocks and a dead-zone block. Input-voltage saturation block, i.e. 27 volts, models the limit on the controller command. Limited torque of the motor is modelled by the saturation on the motor current, i.e. 2 amperes, which also models the nonlinear relationship between magnetic flux and coil current of the motor. The stiction friction is modelled by a dead-zone block at the input of the gimbal, i.e. 0.084 Newton-meter. Viscous friction is included in gimbal model, too. The gyroscope is modelled by a first-order low-pass filter with cut-off frequency of 335 Hertz.

In order to design the controller, a linear model is required to describe the nonlinear system of Figure (2). The nominal model of the system and its multiplicative uncertainty are calculated using well-known closed-loop identification algorithm, i.e. Prediction Error Model (PEM). The third-order identified state-space nominal model of Figure (2) is

$$\begin{pmatrix} \dot{x} \\ y \end{pmatrix} = \begin{pmatrix} -76.06 & 62.6 & 76.68 & 4.161 \\ -313 & -937.7 & 885.4 & 79.1 \\ -345.9 & -1214 & -1138 & 216 \\ 6.628 & -0.0483 & 0.01648 & 0 \end{pmatrix}\begin{pmatrix} x \\ u \end{pmatrix} \tag{42}$$

and its associated multiplicative uncertainty is

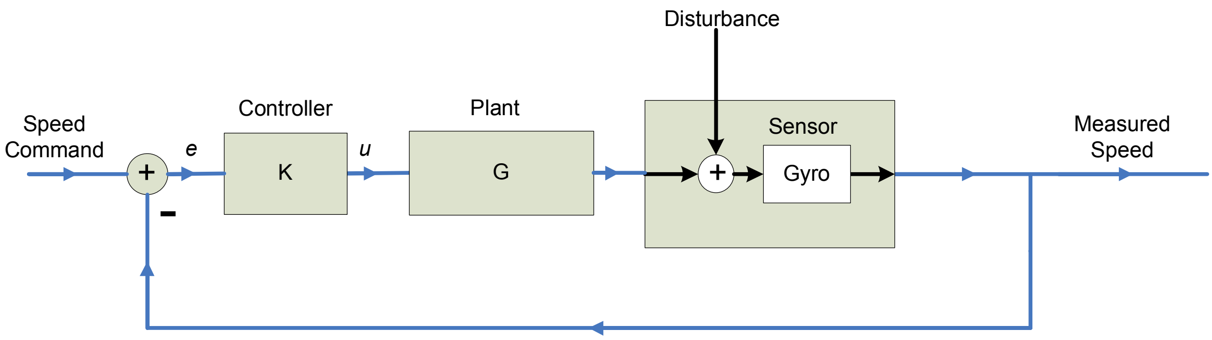

Fig. 1. Block diagram of the stabilization loop.

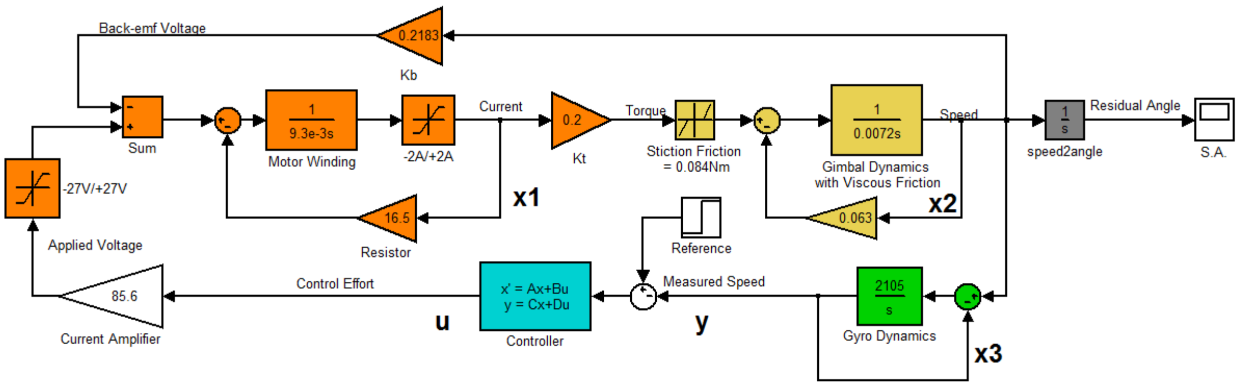

Fig. 2. Investigated model in details.

$$W(s) = 0.0006s + 0.754 \tag{43}$$

If the nominal model is extracted using white-box modelling methods then the states are motor current, gimbal speed and measured (gyroscope) speed as shown in Figure (2). Since, the nominal model (42) is extracted using identification method, its states do not show any physical parameter and they are a combination of physical states (e.g. similar to (Moorty 2002)).

The main goal of the stabilizer controller is to attenuate persistent disturbances in frequency range between 1 Hertz and 10 Hertz while having zero steady state error to step command. This goal is achieved using following weighting functions which are selected by the procedure used in (Moorty 2002).

$$W_s(s) = 0.4\frac{(s+2500)^2}{(s+0.0001)(s+5000)} \tag{44}$$

$$W_u(s) = 0.5 \tag{45}$$

$$W_T(s) = 0.932\frac{s^2+377s+222100}{s^2+3000s+2250253} \tag{46}$$

$W_s(s)$, $W_u(s)$ and $W_T(s)$ are weights for sensitivity, control effort and complementary sensitivity, respectively. In order to achieve zero steady state error a pole close to the origin is added to $W_s(s)$. $W_u(s)$ and $W_T(s)$ limits control effort and closed-loop bandwidth, respectively. Note that the closed-loop system is robustly stable if $min\{W, W_s\} < 1$.

Figure 3 shows the block diagram of the mixed sensitivity problem. The L_1 problem can be stated as

$$\underset{K_{L_1} stabilizing}{find} \quad \|T_{zw}\|_{\infty,\infty} \le \gamma_1 > 0$$

Where

$$T_{zw}(s) = \begin{bmatrix} W_s(1+GK)^{-1} \\ W_uK(1+GK)^{-1} \\ W_TGK(1+GK)^{-1} \end{bmatrix} \tag{47}$$

The problem is solved for the generalized plant P which is given by

$$P = \begin{bmatrix} W_s & -W_sG \\ 0 & W_u \\ 0 & W_TG \\ I & -G \end{bmatrix} \tag{48}$$

The generalized plant (48) for nominal model (42) and weighting functions (44)-(46) is of order seven. In the analysis step, LMIs (14), (15), (16) and (18) are solvable for $\lambda = 1e-9$, simultaneously. So, the controller exists. Assuming that $n = n_k = 7$ and using equation (40), X_2 and consequently X_{cl} are computed. In the synthesis step, LMIs (10) and (17) are solved to find the controller. Solver settings are provided in Table 1 for analysis and synthesis steps. Matrices of the L_1 controller are as follows:

$$A_{K_{L_1}} = \begin{bmatrix} -154.8 & -259.8 & 127.7 & -180.7 & -838.2 & -618.9 & -13.64 \\ -176.4 & -294 & -41.17 & -345.6 & -958.8 & -744.1 & -15.3 \\ -10.17 & 157.4 & -4945 & 390.7 & -442.9 & -22.63 & -5.981 \\ -65.22 & 273.9 & 219.2 & -2464 & 977.3 & -326.2 & -11.07 \\ -12.74 & -94.62 & -309.8 & -1273 & -188.2 & -200.9 & 6.243 \\ -30.91 & -392.8 & -22.48 & -953.3 & -566.4 & -1843 & 78.24 \\ -0.7221 & -20.81 & 1.608 & -1.023 & -15.19 & -81.23 & -1579 \end{bmatrix}$$

$$B_{K_{L_1}} = [-168.1 \quad -213.2 \quad -53.39 \quad -172.7 \quad -0.438 \quad 35.81 \quad 3.456]^T$$

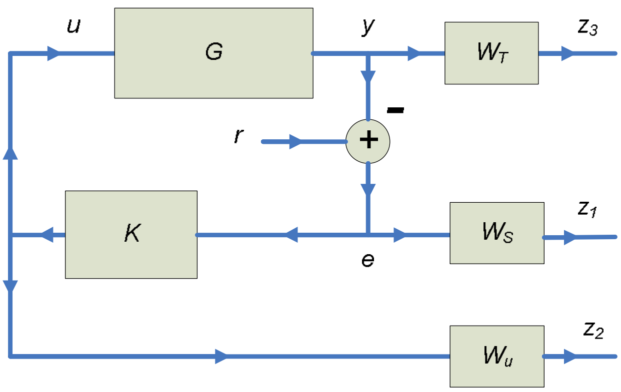

Fig. 3. Mixed sensitivity problem structure.

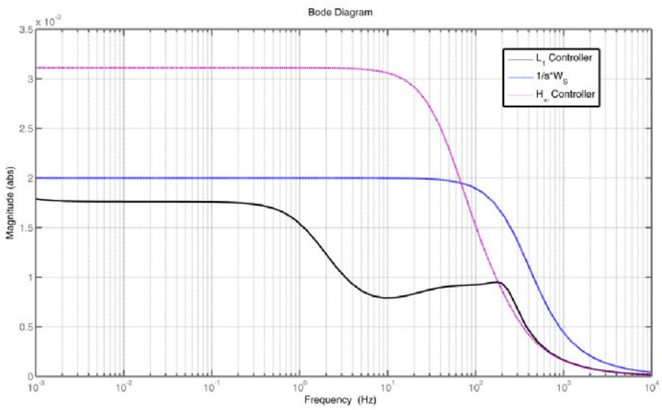

Fig. 4. Attenuation curves.

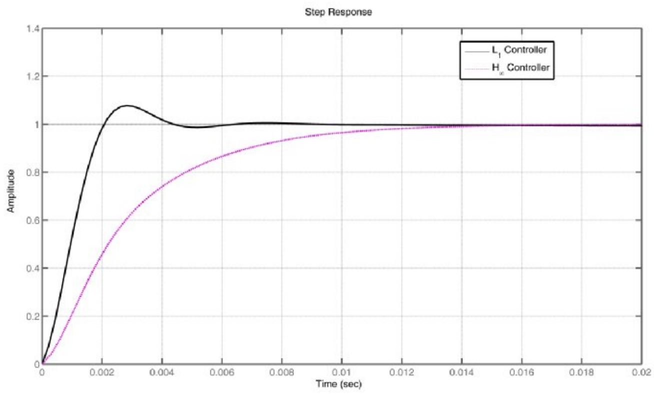

Fig. 5. Step responses with original controllers.

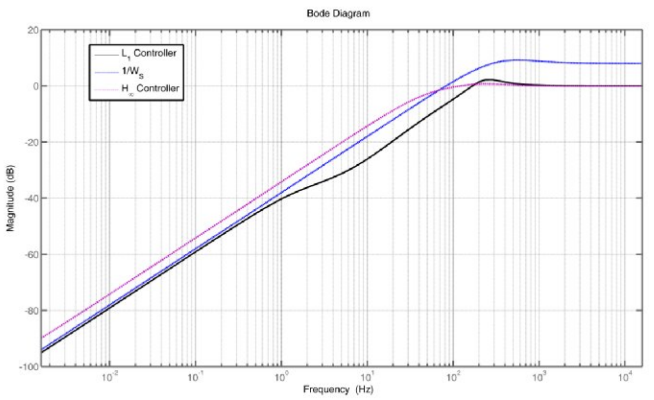

Fig. 6. Achieved sensitivity functions.

$$\mathrm{C}_{\mathrm{K}_{\mathrm{L}_1}} = [7.449 \quad 7.444 \quad -5.146 \quad 17.64 \quad 40.02 \quad 32.1 \quad 0.6361]$$

$$\mathrm{D}_{\mathrm{K}_{\mathrm{L}_1}} = 9.231$$

The L_1 controller is compared with an H_∞ controller (from reference (Moorty 2002)) using the step response and the stability accuracy. The H_∞ controller is designed by the same generalized plant so the controller is of order 7. The controller is as follows:

$$\mathrm{A}_{\mathrm{K}_{\mathrm{H}_\infty}} = \begin{bmatrix} -10864767 & 6919861 & -87582 & 8365.9 & 65233 & 3269 & 340 \\ -12386971 & 7889361 & -100038 & 9411.2 & 74369 & 3692 & 388 \\ -713771.8 & 454502 & -10651 & 1446.5 & 3879 & 360 & 16 \\ -4578655 & 2916157 & -36662 & 1861.9 & 28795 & 1499 & 136 \\ -894622.9 & 569781 & -7544 & -678.6 & 5256 & 90 & 35 \\ -2170236 & 1382225 & -17606 & 180.4 & 12652 & -1214 & 150 \\ -50691.7 & 32285.6 & -411.4 & 4.8 & 294 & -71 & -1577 \end{bmatrix}$$

$$\mathrm{B}_{\mathrm{K}_{\mathrm{H}_\infty}} = [-20.517 \quad -0.86 \quad -24.69 \quad 2.229 \quad -1.057 \quad 0.0439 \quad 0.00001]^{\mathrm{T}}$$

$$\mathrm{C}_{\mathrm{K}_{\mathrm{H}_\infty}} = [-462109.7 \quad 294325 \quad -3725.8 \quad 349.77 \quad 2774.8 \quad 137.5 \quad 14.5]$$

$$\mathrm{D}_{\mathrm{K}_{\mathrm{H}_\infty}} = 0$$

Table 1. Solver settings.

	Analysis Step	Synthesis Step
Solver	sdpt3	lmilab
Feasibility radius	1e2	1e4
Tolerance	1e-10	1e-9
Maximum iterations	1e4	1e2

4. NUMERICAL SIMULATIONS

In this section, some simulations are done to show the efficiency of the proposed controller in comparison with the H_∞ controller. For comparison, a method is required for measuring the stability accuracy of the system. There are two kinds of criteria for measuring the stability accuracy of a system including frequency-domain criterion and time-domain criterion.

One of the frequency domain criteria is the attenuation curve (e.g. (Moorty 2002)). The attenuation curve shows the amount of attenuation from persistent speed disturbances to the output angle for sine-wave disturbances with different frequencies. The minimum attenuation of the closed-loop system is equal to the H_∞ norm of the attenuation transfer function. However, the peak of the attenuation of the closed-loop system should be computed by the $\mathcal{L}_\infty$-induced norm which is more than the H_∞ norm. In order to have more information about the amount of attenuation, one should plot the attenuation over frequency. Attenuation curve is a suitable tool for controller design and performance analysis of random disturbances.

A time-domain criteria is the single-frequency sine-wave excitation (Ji 2011, Kennedy 2003). To measure the stability accuracy, the system is excited by a sine-wave disturbance and residual angle is measured. The frequency and amplitude of the sine-wave depends on the type and movement of the vehicle which carries the system. For example, if the gyro-stabilized system is going to be mounted on a helicopter then a sine-wave with frequency between 10 to 50Hz and amplitude of 15 deg/s or less may be a good choice for excitation signal. For a land vehicle, a good signal may have the frequency less than 5Hz with amplitude more than 20 deg/s.

The attenuation curves for two controllers and the desired one are plotted in Figure 4. This figure illustrates that the L_1 controller attenuates disturbances better than the H_∞ controller. For the closed-loop system with L_1 controller one has

$$\|att_{L_1}\|_1=1.988e\text{-}3 \quad \text{and} \quad \|att_{L_1}\|_\infty=1.76e\text{-}3$$

and for the closed-loop system with H_∞ controller one has

$$\|att_{H\infty}\|_1=3.112e\text{-}3 \quad \text{and} \quad \|att_{H\infty}\|_\infty=3.11e\text{-}3$$

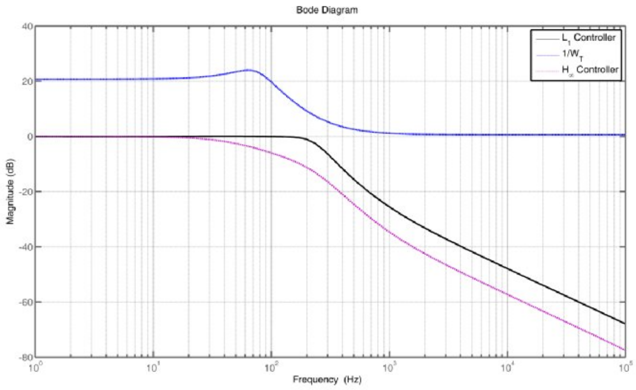

Fig. 7. Achieved complementary sensitivity functions.

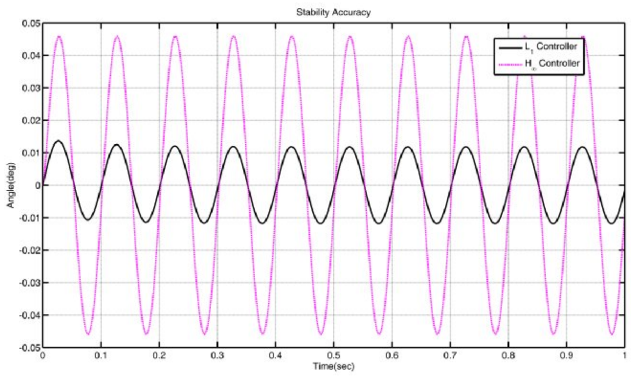

Fig. 8. Achieved stability accuracy.

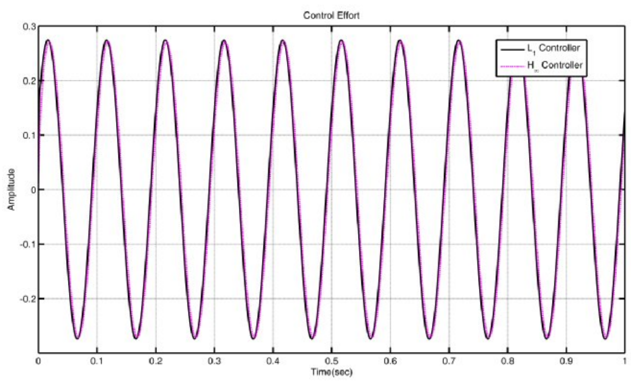

Fig. 9. Control efforts.

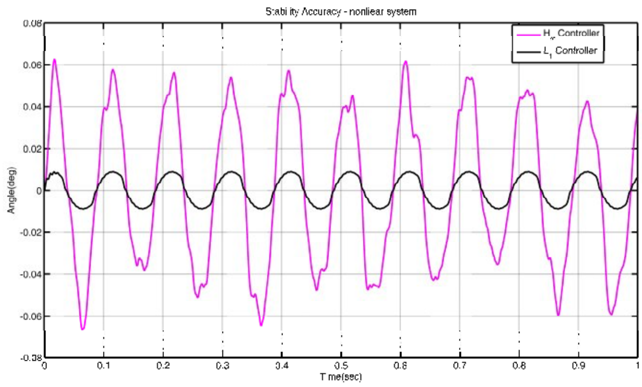

Fig. 10. Achieved stability accuracy – nonlinear system.

Comparing above values indicates that the L_1 controller works better than the other one.

The step responses are compared in Figure 5. The rise time for the closed-loop system with the L_1 controller is less than 2ms and its overshoot is about 8 percent. The rise time of the closed-loop system with the H_∞ controller is about 10ms and there is no overshoot.

Figure 6 shows achieved sensitivity functions for the controllers and $W_s^{-1}(s)$. The 0-dB cross over frequencies of the sensitivities are 180Hz and 120Hz for the L_1 controller and the H_∞ controller, respectively. It can be observed that the achieved sensitivity of the H_∞ controller is greater than that of the L_1 controller and the $W_s^{-1}(s)$. The achieved closed-loop plots and the $W_T^{-1}(s)$ are shown in Figure 7. According to the plots, the closed-loop bandwidths are 240Hz and 55Hz for the L_1 controller and the H_∞ controller, respectively.

The stability accuracy of the linear closed-loop systems are plotted in Figure 8, for sine-wave with frequency of 10Hz and amplitude of 15deg/s. The stability accuracy of the close-loop system with the H_∞ controller is about 785 micro radians while that of the L_1 controller is less than 227 micro radians. Hence, the stability accuracy of the platform improves more than three times using the proposed controller. Figure 9 shows the control efforts. It demonstrates that improvement in the stability accuracy is achieved with no more control effort. Figure 10 contains the stability accuracy for nonlinear system shown in Figure 2. The plots are similar to the plots of Figure 8.

Simulations of this section show that the introduced controller works better than the $_\infty$ controller both in time domain and frequency domain. It should be mentioned that the superiority of the $_1$ controller is not a universal superiority and it is due to the special application of the controller for inertial stabilization problem. The number of operations required to design the proposed controller is usually more than the other one but the processing time is the same in the implementation.

5. CONCLUSION

In this article, a robust L1 controller is designed for inertial stabilization of a nonlinear platform. The controller is designed using four Linear Matrix Inequalities (LMIs). The algorithm is the modified one and the analysis and synthesis steps are completely separated. Consequently, the original algorithm can be applied to more problems. The performance of the proposed controller is evaluated using simulation. Results show that the L1 controller improves the accuracy of stabilization in comparison with an H_∞ controller while the closed-loop system is robustly stable.

REFERENCES

Gahinet, P., and P. Apkarian, "A linear matrix inequality approach to H∞ control", Int. J. Robust Nonlinear Control, vol.4, pp. 421-448, 1994

Hilkert, J.M., ''Inertially stabilized platform technology'' IEEE Cont. Sys. Magazine, pp. 26-46, 2008

Ji, W., Q. Li, B. Xu, D. Zhao and S. Fang, ''Adaptive fuzzy PID composite controller with hysteresis-band switching for line of sight stabilization servo system'', Aerospace Science and Technology, 15, pp. 25-32, 2011

Kennedy, P.J., and R.L. Kennedy, "Direct versus indirect line of sight (LOS) stabilization", IEEE Trans. Control System Tech., 11, pp. 3-15, 2003

Khosravi, A., and A.A. Jalali, "A new LMI solution in the L1 optimal problem for wind turbine-induction generator unit", Applied Math. Computation, 206(2), pp. 643-650, 2008

Lee, T.H., S.S. Ge and C.P. Wong, "Adaptive neural network feedback control of a passive line-of-sight stabilization system", Mechatronics, Vol. 8, pp.887-903, 1998

Li, B., D. Hullender and M. DiRenzo, ''Nonlinear Induced Disturbance Rejection in Inertial Stabilization System'', IEEE Trans. Control Systems Tech., Vol 3, pp. 421-427, 1998a

Li, B., and D. Hullender, ''Self-tuning controller for nonlinear inertial stabilization system'', IEEE transaction on control system technology, Vol. 6, No. 3, pp. 428-434, 1998b

Moorty, J.A.R.K. R., Marathe and V.R. Sule, "H∞ control law for line-of-sight stabilization for mobile land vehicles", Optical Engineering, 41(11), pp. 2935-2944, 2002

Moorty, J.A.R. K., R. Marathe and H. Babu, ''Fuzzy controller for line of sight stabilization systems'', Optical Engineering, Vol. 43(6), pp.1394-1400, 2004

Ortega, J.J., ''Gunfire performance of stabilization electro-optical sights'', Proc. SPIE, 3692, pp.74-83, 1999

Packard, A., K. Zhou, P. Pandey and G. Becker, "A collection of robust control problems leading to LMI's", Proc. CDC, pp. 1245-1250, 1991

Rezac, M., and Z. Hurak, 'Vibration rejection for inertially stabilized double gimbal platform using acceleration feedforward' IEEE CCA, pp. 363-368, 2011

Rue, A.K., ''Stabilization of precision electro-optical pointing and tracking systems'', IEEE transaction on Aerospace and electronic systems, Vol. AES-5, pp. 805-819, 1969

Rue, A.K., ''Precision stabilization systems'', IEEE Trans. Aerospace and Electronic systems, Vol. AES-10, pp. 34-42, 1974

Sherer, C., and S. Weiland, Linear Matrix Inequality in Control, Delft University of Technology, the Netherlands, Dec. 9 2004

Seong, K.J., H.G. Kang, B.Y. Yeo, and H.P. Lee, ''The stabilization loop design for a two-axis gimbal system using LQG/LTR controller'', SICE-ICASE Inter. Joint Conf., pp.18-21, 2006

Wang, L., M. Ling, D. Wang, Y. Chen and C. Wang, "Line-of-Sight Stabilization System Based on Fractional-Order Control", Proc. IEEE, pp. 828-831, 2008